

Application of full and approximate flow models in topology optimisation of passive cooling for electronics cabinets

Joe Alexandersen
Department of Technology and Innovation
University of Southern Denmark
DK-5230 Odense M, Denmark
Email: joal@iti.sdu.dk

ABSTRACT

This paper applies a previously developed framework for topology optimisation of passive cooling to a vertically-oriented electronics cabinet with multiple heat generating chips. The flow field in the cabinet is complex due to the buoyancy generated by the multiple chips interacting with each other. Thus, it becomes difficult to intuitively design heat sinks for this application. Therefore, topology optimisation is applied to generate optimised heat sink geometries customised for the actual layout of chips inside the cabinet. Both a full Navier-Stokes flow model and an approximate flow model is applied to the problem. The approximate model is shown to be insufficient on its own for the defined problem and the full model is shown to be computationally expensive and unstable. A hybrid optimisation approach is then applied, using the full model in the beginning to point the optimisation in the right direction and the approximate model in the subsequent stages to fine tune the heat sink designs. The full model is shown to introduce flow-aware features in the heat sink designs, that increase the performance substantially. It is concluded that heat sink designs should be different for each of the chips in the cabinet depending on its location and interaction with the thermal plumes from other chips.

KEY WORDS: topology optimisation, heat sink design, electronics cooling, reduced model, potential flow, surrogate model

NOMENCLATURE

c_p	specific heat capacity [J/(kg °C)]
\mathbf{g}	gravitational acceleration [m/s ²]
k	thermal conductivity [W/(m °C)]
p	pressure field [Pa]
q	penalisation factor
s	volumetric heat generation [W/m ³]
T	temperature field [°C]
\mathbf{u}	velocity field [m/s]
\mathbf{x}	spatial coordinate [m]
A	approximate model
NS	Navier-Stokes model

Greek symbols

α	Brinkman penalisation/impermeability [m ²]
β	thermal expansion coefficient [1/°C]
γ	design field
μ	dynamic viscosity [Pa s]
$\bar{\mu}$	artificial material parameter [kg/(m ³ s)]
ρ	mass density [kg/m ³]
ω	heat generating domain
Ω	computational domain

Subscripts

f	fluid
i	spatial dimension, $i \in \{1,2,3\}$
max	maximum value
s	solid
0	reference value

INTRODUCTION

Passive cooling can be used to cool electronics components without the addition of an external active flow driver, such as a fan or pump. Passive cooling exploits the natural fluid circulation arising from buoyancy through density differences due to spatial temperature gradients. Thus, the cooling is passive because it utilises the natural fluid motion and it is “free” because it exploits the already wasted thermal energy to drive the cooling flow.

Topology optimisation is a structural design method originating from solid mechanics, where the stiffness of a structure is maximised by distributing material as to minimise the local strain energy [1, 2]. During the past decades, topology optimisation has been extended to a wide array of physics [3]. Borrvall and Petersson [4] published the seminal work on topology optimisation for Stokes flow problems, which was subsequently extended to Navier-Stokes flow [5, 6]. The application of topology optimisation for forced convection conjugate heat transfer followed soon after [7, 8] with many new contributions this past decade [9]. Considering passive cooling, Alexandersen et al. [10] presented the first application of topology optimisation for natural convection. This has subsequently been extended to large scale three-dimensional problems [11] and applied to the design of passive coolers for light-emitting diode lamps [12]. The optimised designs were experimentally shown to be superior to standard pin-fin designs by manufacturing the optimised designs using metallic additive manufacturing [13] and investment casting [14].

Simulating the full passive conjugate heat transfer problem is computationally expensive, especially in the context of optimisation. Firstly, one must simulate the Navier-Stokes equations with a two-way coupling to the thermal convection-diffusion equation through the temperature-dependent density. When discretised, this yields a large non-linear system of equations with 5 degrees of freedom in three spatial dimensions (3 velocity, 1 pressure, 1 temperature). Secondly, due to the iterative nature of numerical optimisation, the simulation is repeated hundreds to thousands of times during the optimisation process. Thus, it becomes relevant to use approximate models. The simplest method is to reduce the convective cooling into a convective boundary condition based on Newton’s law of

cooling [15-18]. However, this crude approximation can lead to many problems and non-physical artefacts [15, 17-20].

Recently, Joo et al. [21, 22] presented an extension to this method, where the distance between conductive members is calculated using a global search of interface elements and this is subsequently used in calculating the spatially-varying convection coefficient based on correlations. This method seems to be successful in introducing some knowledge of the flow into the optimisation process, but it requires the choice of relevant correlations based on *a priori* assumptions of the geometry.

Therefore, the author and co-workers have proposed an approximate flow model [20, 23] for natural convection problems. The model, which is a potential flow-like model, is used in this work. The method is similar to Darcy's law for flow through a porous medium, but in the fluid regions an artificial material parameter must be tuned to approximate the full Navier-Stokes flow solution. The method introduces design, geometry and orientation dependent effects in the convective modelling at a significantly reduced computational cost. However, as will be shown in this paper, this approximate model also has its limitations.

CONJUGATE HEAT TRANSFER MODEL

In order to simulate conjugate heat transfer, the governing equation is a unified version of the convection-diffusion equation:

$$\rho c_p u_i \frac{\partial T}{\partial x_i} - \frac{\partial}{\partial x_i} \left(k(\mathbf{x}) \frac{\partial T}{\partial x_i} \right) = s(\mathbf{x})$$

where T is the temperature field, ρ is the material density, c_p is the specific heat capacity, k is the thermal conductivity, and s_T is the volumetric heat generation. Lastly, \mathbf{x} is the coordinate vector and \mathbf{u} is the velocity vector field, both of which consist of three components, x_i and u_i where $i \in \{1,2,3\}$. The velocity field needs to be found in order to simulate the convective heat transfer in the conjugate heat transfer problem. Herein the fluid velocity is governed by either a full model, the Navier-Stokes equations, or an approximate model, a potential-like flow model – both of which will be discussed in the next section.

For conjugate heat transfer, the computational domain Ω is composed of two subdomains:

$$\Omega = \Omega_f \cup \Omega_s$$

where Ω_f is the fluid domain and Ω_s is the solid domain. The thermal conductivity varies in the two subdomains as:

$$k(\mathbf{x}) = \begin{cases} k_f & \text{if } \mathbf{x} \in \Omega_f \\ k_s & \text{if } \mathbf{x} \in \Omega_s \end{cases}$$

where k_f and k_s are the thermal conductivity of the fluid and solid, respectively. The volumetric heat generation is only active in a predefined subdomain of the solid domain, $\omega \subset \Omega_s$, modelling one or multiple electronics chips:

$$s(\mathbf{x}) = \begin{cases} 0 & \text{if } \mathbf{x} \notin \omega \\ s_\omega & \text{if } \mathbf{x} \in \omega \end{cases}$$

It is further assumed that the velocity field is zero, or at least numerically insignificant, inside the solid domain:

$$u_i(\mathbf{x}) \approx 0 \text{ if } \mathbf{x} \in \Omega_s$$

Thus, the convective term disappears and only conduction exists in the solid domain.

FULL AND APPROXIMATE FLOW MODELS

In order to simulate the conjugate heat transfer, solving for the temperature field in both the fluid and solid domains, the fluid velocity field must be calculated. In this section, the two different models used will be described. For both models, the Boussinesq approximation is introduced to include density variations due to temperature in the buoyancy term, allowing to model passive cooling through natural convection:

$$\rho \mathbf{g} \approx \rho_0 (1 - \beta(T - T_0)) \mathbf{g}$$

where β is the volumetric thermal expansion coefficient, ρ_0 and T_0 are the reference density and temperature, respectively, and \mathbf{g} is the gravitational acceleration vector.

Full model: Navier-Stokes equations

The Navier-Stokes equations are the most general governing equations of fluid flow. Here they are posed in the steady-state form under the assumption of constant fluid properties:

$$\rho_0 u_j \frac{\partial u_i}{\partial x_j} - \mu \frac{\partial}{\partial x_j} \left(\frac{\partial u_i}{\partial x_j} + \frac{\partial u_j}{\partial x_i} \right) + \frac{\partial p}{\partial x_i} = -\alpha(\mathbf{x}) u_i - \rho_0 \beta g_i (T - T_0)$$

where p is the pressure field and μ is the dynamic viscosity. On the right-hand side there are two force terms: the first is a Brinkman penalisation term; and the second is the buoyancy term due to the Boussinesq approximation. Brinkman penalisation is used to ensure numerically insignificant velocities inside the solid domain and free flow in the fluid domain, by varying the Brinkman penalisation coefficient, α :

$$\alpha(\mathbf{x}) = \begin{cases} 0 & \text{if } \mathbf{x} \in \Omega_f \\ \alpha_{\max} & \text{if } \mathbf{x} \in \Omega_s \end{cases}$$

The Navier-Stokes equations are a set of non-linear coupled partial differential equations. Therefore, they are computationally expensive to solve, and large computational clusters are necessary to solve large three-dimensional problems with high-resolution discretisations. Therefore, for optimisation, which is an iterative process with hundreds to thousands of design iterations, it is of interest to use approximate models that significantly reduce the work load.

Approximate model: potential flow model

The approximate model used in this work has previously been presented for topology optimization of single heat sinks passively cooled by natural convection in enclosures [20, 23]. The detailed derivation, including assumptions and arguments, is presented therein and will not be repeated in this work.

The governing equation for the fluid pressure is:

$$\frac{\partial^2 p}{\partial x_i \partial x_i} = -\rho_0 \beta g_i \frac{\partial T}{\partial x_i}$$

with the fluid velocity defined explicitly by:

$$u_i = -\frac{1}{\bar{\mu}(\mathbf{x})} \left(\frac{\partial p}{\partial x_i} + \rho_0 \beta g_i (T - T_0) \right)$$

The defining material parameter, $\bar{\mu}(\mathbf{x})$, is artificial and is defined by:

$$\bar{\mu}(\mathbf{x}) = \begin{cases} \bar{\mu}_f & \text{if } \mathbf{x} \in \Omega_f \\ \frac{\mu}{\alpha_{\max}} & \text{if } \mathbf{x} \in \Omega_s \end{cases}$$

where the value in the solid is chosen to be consistent with the Brinkman penalisation of the Navier-Stokes model. The value

in the fluid domain, $\bar{\mu}_f$, is defined based on the analytical tuning procedure proposed by Pollini et al. [23] yielding:

$$\bar{\mu}_f = 10^{-4} \text{ kg}/(\text{m}^3 \text{ s})$$

The approximate flow model is a linear equation for the fluid pressure, with the velocities found explicitly after solving for the pressure field. Therefore, the number of degrees of freedom per node has been decreased to just 1, rather than 3, in turn giving a significant reduction in computational cost.

TOPOLOGY OPTIMISATION OF PASSIVE COOLING

A design field, $\gamma(\mathbf{x})$, is introduced which defines which points in space is defined as solid or fluid:

$$\gamma(\mathbf{x}) = \begin{cases} 1 & \text{if } \mathbf{x} \in \Omega_f \\ 0 & \text{if } \mathbf{x} \in \Omega_s \end{cases}$$

In order to perform gradient-based topology optimisation using a density-based formulation, this field is allowed to continuously vary between 0 and 1 at all points. In order to ensure the correct governing equations in each material subdomain, interpolation functions are introduced for the material properties that vary between the solid and fluid domains. Furthermore, density filtering is used to impose a minimum design length scale [24].

Material property interpolation

The three defining material parameters are the conductivity, $k(\mathbf{x})$, the Brinkman penalisation, $\alpha(\mathbf{x})$, and the artificial material parameter, $\bar{\mu}(\mathbf{x})$. These are interpolated as follows:

$$k(\mathbf{x}) = k_f + \frac{\gamma(\mathbf{x})}{1 + q_k(1 - \gamma(\mathbf{x}))} (k_s - k_f)$$

$$\alpha(\mathbf{x}) = \alpha_{\max} \frac{1 - \gamma(\mathbf{x})}{1 + q_\alpha \gamma(\mathbf{x})}$$

$$\bar{\mu}(\mathbf{x}) = \frac{q_{\bar{\mu}} \gamma(\mathbf{x}) + 1}{\bar{\mu}_f + \gamma(\mathbf{x})(\bar{\mu}_s(q_{\bar{\mu}} + 1) - \bar{\mu}_f)}$$

where the penalisation of intermediate design field values is controlled using the penalisation factors: q_k , q_α and $q_{\bar{\mu}}$.

Hybrid optimisation approach

In contrast to standard engineering practise, where the fidelity of a model is often refined over the design/optimisation process in order to save time in the initial stages, a flipped approach was introduced by Pollini et al. [23]. Here the full model is used for the initial stages of the optimisation process in order to push the design in the right direction. Thereafter, a switch to the approximate model allows for polishing off the design during the final stages at a vastly reduced computational cost. The same approach is taken in the present work for a variety of reasons as will be discussed later.

Continuation strategy

A continuation strategy on the interpolation parameters is applied in this work, either for a single model or in combination with switching the model type. Based on previous experience [11, 12], the continuation strategy is based on 6 steps with the following values:

$$\begin{aligned} q_k &\in \{1, 10, 100, 100, 100, 100\} \\ \alpha_{\max} &\in \{10^5, 10^5, 10^5, 10^6, 10^7, 10^8\} \\ q_\alpha &\in \{10, 1, 1, 10, 100, 1000\} \\ q_{\bar{\mu}} &\in \{-0.2, 4, 4, 7, 7.89, 7.89\} \end{aligned}$$

The flow model can either be the same throughout or be varied and is denoted using NS for the Navier-Stokes model and A for the approximate model, with the number of continuation steps in brackets. When using the hybrid optimisation approach, where the flow model is switched during the optimisation procedure, the following notation is used: NS(n_{NS})-A(n_{A}), where n_{NS} is the number of Navier-Stokes steps and n_{A} is the number of approximate model steps.

PROBLEM DEFINITION

Fig. 1 shows an illustration of the problem setup. The goal is to design the heat sinks for four identical heat generating chips distributed regularly inside a shallow vertical cabinet with an inlet at the bottom right and an outlet at the top left. The colours denote the following: light grey surfaces are open boundaries; dark grey surfaces are walls (the outer lateral wall is not shown); the red areas are the heat generating chips; and the green areas are the design domains where solid material and fluid can be distributed. The cabinet is 50cm tall, 40cm wide and 10cm deep. The inlet and outlet are each 25cm wide and placed askew from one another, both of them with a zero normal stress condition imposed. The walls have zero velocities for the full model, but only zero normal velocities for the approximate model. Each chip is 10cm tall, 10cm wide, 1cm thick and generates 1W of thermal power. This power level is chosen as it allows for a steady-state solution of the flow and temperature problems. On top of each chip, an 8cm thick design domain is placed. The chips are placed on a non-conducting outer wall (in reality, a circuit board will conduct heat to some degree). All outer walls are assumed insulated, the air at the inlet is 20°C and only convective fluxes exist at the outlet.

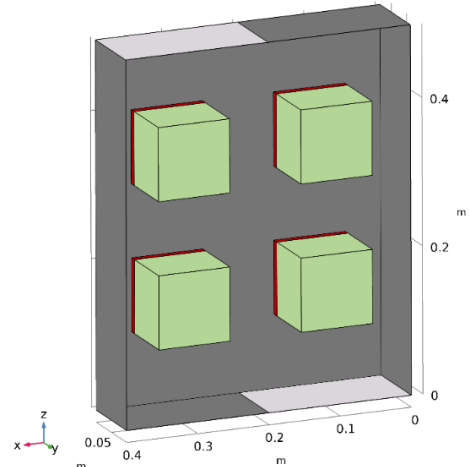


Fig. 1: Illustration of the problem setup.

The optimisation formulation follows that from previous work [20, 23] and is thus not repeated here formally. The objective is to minimise the thermal compliance functional of the system under a global solid volume constraint. This is equivalent to minimising the average temperature of four chips with a constraint on the total volume of solid material used. This means that the solid material can be placed unequally among the four heat sinks in order to benefit the average temperature across all four chips. Here a total volume constraint of 20% of the design domain volume is used, equivalent to 640cm³ distributed over the four heat sinks.

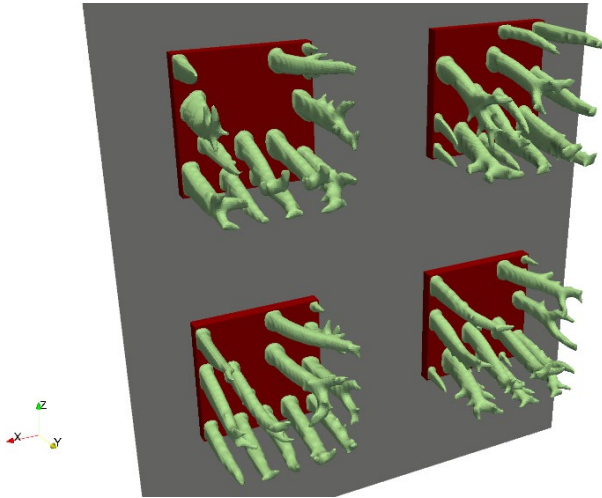


Fig. 2: Optimised heat sink designs using the approximate flow model, A(6).

The computational domain is discretised using $288 \times 72 \times 360$ trilinear elements yielding 38 million DOFs for the full model and 15.2 million DOFs for the approximate model. The minimum design length scale is set to 6.7mm (limited by the mesh resolution). Material properties are defined in Table 1.

Table 1: Values for material properties used in models.

ρ [kg/m ³]	c_p [J/(kg K)]	β [10 ⁻³ /K]	k_s [W/(m K)]	k_f [W/(m K)]	g_i [m/s ²]
1.2	1000	3.69	200	0.02435	{0,0,-1}

RESULTS

Approximate flow model

The optimised heat sink geometries using the approximate flow model (denoted as “A(6)”) can be seen in Fig. 2, where the same colours as previously is used for features. It can be seen that the designs are primarily made up of straight pins of approximately circular cross-sections. There are only few members with secondary branching. The four heat sink designs are visually very similar and interestingly, the solid volume is distributed more or less equally among the four heat sinks with a standard deviation of only 1.3% from the mean.

Navier-Stokes flow model

In addition to the Navier-Stokes model being computationally expensive, the non-linear nature also easily becomes unsteady during the optimisation process causing the steady-state solver to fail. For this problem, it has been observed that the solver fails at the 4th continuation step and cannot continue. This can be because the increasing Brinkman penalisation either causes the system to become ill-conditioned, or more likely the increasingly physical model becomes unsteady for the prescribed settings. Therefore, Fig. 3 shows the

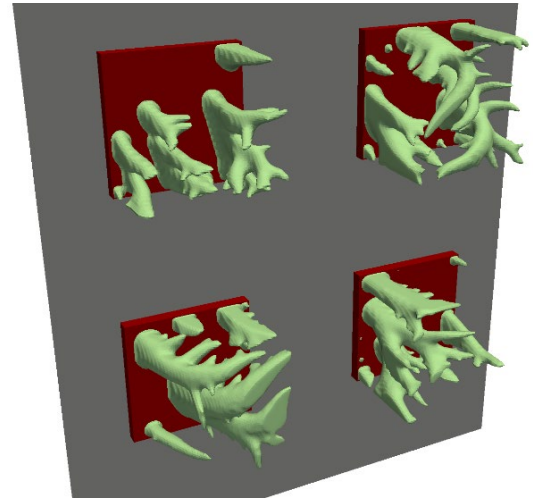


Fig. 3: Optimised heat sink designs using the Navier-Stokes flow model after the 3rd continuation step, NS(3).

optimised heat sink designs at the end of the 3rd continuation step (denotes as “NS(3)”). Here it can easily be seen, that the designs are significantly different to those obtained using the approximate flow model. Here more complex structures are seen with significant curvature and elongated cross-sections.

Validation analyses

In order to validate the performance of the obtained designs using the two models, the designs are imported into the commercial finite element software COMSOL Multiphysics 5.4. An isovolume at a design field value of 0.75 is used for exporting the designs to an STL file¹. Both sets of designs are analysed using a full Navier-Stokes model to see which performs best and to investigate the differences.

The design volume for the approximate flow model is 360.8cm³ and the mean temperature is 3.379°C. For the Navier-Stokes flow model, the design volume is 441.3cm³ and the mean temperature is 2.758°C. The mean temperature of the Navier-Stokes design is significantly lower than that obtained using the approximate model. This indicates that the approximate model is insufficient as a surrogate when optimising the specified problem. The larger design volume of the Navier-Stokes design can possibly also contribute to the better performance².

Fig. 4 shows the vertical mid-XZ-plane used for plotting velocities and temperatures in the following figures.

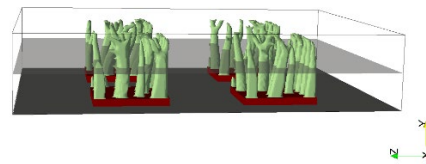


Fig. 4: Vertical mid-XZ-plane used for plotting velocities and temperature fields.

¹ This value is chosen based on trial-and-error to produce a good equivalence between the physical models of the continuous design field and discrete surface representations [11].

² The difference in volume is due to the different stages in the design process the extracted designs are taken from: the Navier-Stokes design is from the 3rd continuation step, where significant intermediate design field values still exist and, thus, more grey material is promoted to fully solid in the isovolume process.

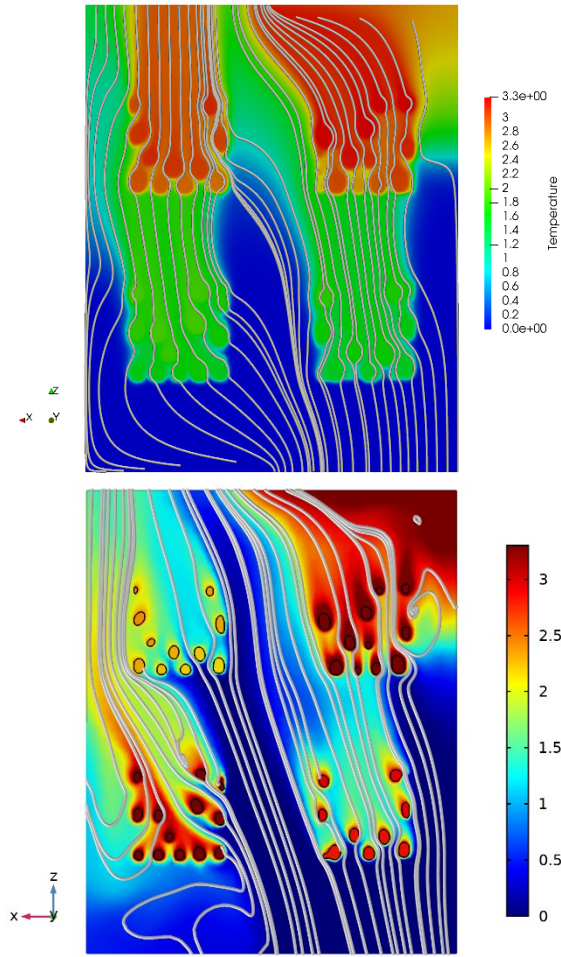


Fig. 5: Temperature field and in-plane streamlines of the vertical mid-XZ-plane for the A(6) design using the approximate model from in-house code (top) and the Navier-Stokes model in COMSOL (bottom).

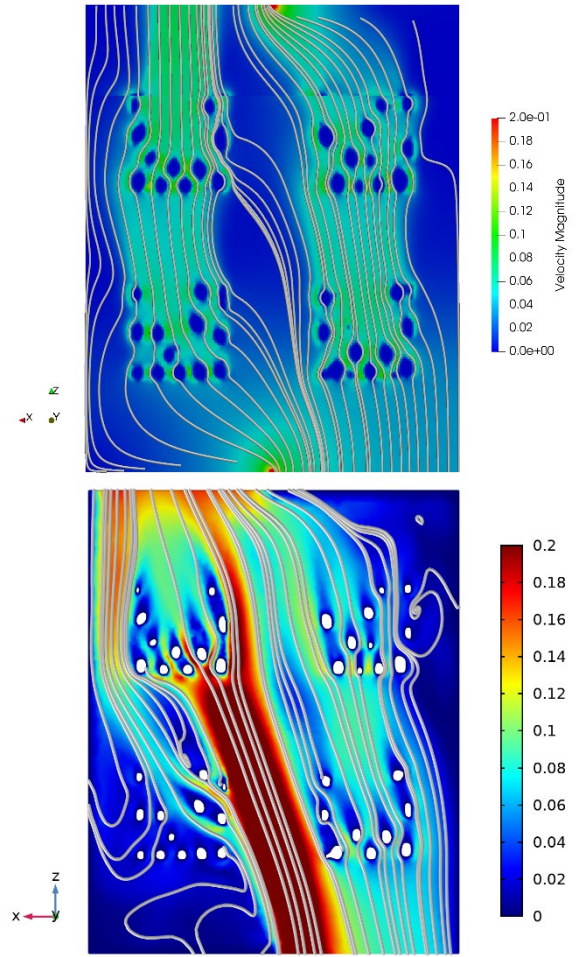


Fig. 6: Velocity field and in-plane streamlines of the vertical mid-XZ-plane for the A(6) design using the approximate model from in-house code (top) and the Navier-Stokes model in COMSOL (bottom).

Fig. 4 shows the temperature field and in-plane streamlines of the vertical mid-XZ-plane using the approximate model in the developed in-house code (top) and a Navier-Stokes validation model in COMSOL (bottom). It is seen that there are vast differences between the predictions of the two models. The approximate model predicts a more even distribution of the cool air across the bottom of the cabinet, causing the two bottom chips to have lower temperatures than the two at the top, because they receive “old” warm air from those directly below. In contrast, using the Navier-Stokes flow model it is observed that the two chips in the diagonal from inlet to outlet (bottom right to top left) are the coolest. This is further exemplified by the respective flow fields shown in Fig. 5, where it is clearly seen that the Navier-Stokes model has a main flow from the inlet to the outlet where the highest velocities are found. In contrast, the highest velocities for the approximate model are found between the members of the heat sinks (if the singularity at the inlet and outlet edges are neglected). It is clear that the potential-driven nature of the approximate model causes the flow to distribute more evenly along the horizontal direction. This is because the model lacks inertia, which causes the real flow to be fastest in the diagonal from inlet to outlet. Furthermore, it is observed that the lack of a viscous boundary

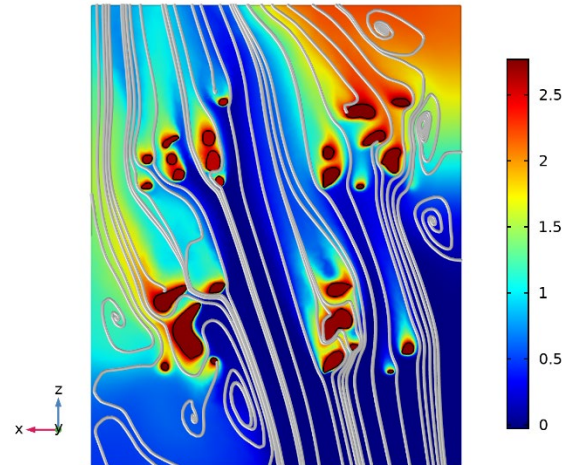


Fig. 7: Temperature field and in-plane streamlines of the vertical mid-XZ-plane for the NS(3) design using COMSOL.

layer at the outer walls and, thus, a slip wall condition also contributes to a large error. This is most likely more important in the present problem, compared to earlier examples [23], due

to the outer walls of the cabinet being very close to the design domain.

To investigate the difference in performance for the designs optimised using the approximate and Navier-Stokes models, the temperature field for the Navier-Stokes based design (after 3 continuation steps) is shown in Fig. 6. Here it can be seen, that the design features seem to change the flow pattern such that reuse of already heated air is reduced. This allows the cool air flow to reach more of the upper heat sinks. In contrast to the designs based on the approximate model, the volume used for each heat sink is very different: the upper left heat sink uses the least material with only 19.6% of the total material used; the lower right heat sink uses the second least material with 24.4%; the upper right uses the second most material with 27.5%; and the lower left uses the most material with 28.5%. Interestingly it is the off-diagonal heat sinks that use the most material, most likely because they are not exposed to as much cool air due to the main diagonal flow from inlet to outlet.

Hybrid optimisation approach

Due to the poor performance obtained using the approximate model, the instabilities observed in the latter stages for the full model, and to speed up the optimisation process, the hybrid optimisation approach is now applied to the problem. Two model configurations are used: NS(1)-A(5) consisting of 1 initial continuation step using Navier-Stokes and subsequently 5 continuation steps using the approximate model; and NS(2)-A(4) consisting of 2 initial continuation steps using Navier-Stokes and subsequently 4 continuation steps using the approximate model.

Figs. 7 and 8 show the optimised heat sink designs using the two model configurations using the hybrid optimisation approach. Compared to the designs obtained using only the approximate model, Fig. 2, it can be seen that the ones obtained using the hybrid approach retain more of the flow-informed complexities from the Navier-Stokes designs, Fig. 3, generated during the initial stages using the Navier-Stokes model. It can be concluded that the curved members and clear flow paths are found during the initial stages of the optimisation, but that the approximate model can be used to polish off the results. It is

Table 2: Mean temperatures, total design volumes and computational time (core-hours) for model configurations.

Model configuration	Mean temperature [°C]	Design volume [cm ³]	Core-hours
A(6)	3.379	360.8	909
NS(1)-A(5)	2.666	377.9	11051
NS(2)-A(4)	2.654	379.3	23147
NS(2)	2.765	430.2	22411
NS(3)	2.758	441.3	30984

interesting to note, that no instabilities were observed when using the approximate model, even for a large solid impermeability.

Table 2 lists the mean temperatures, total design volumes and computational time used (in terms of core-hours) for five different model configurations. In addition to the four previously presented, the design after 2 continuation steps using Navier-Stokes, NS(2), has also been analysed in COMSOL. The designs using the approximate model only, A(6), is seen to perform significantly worse than all the others. The best performing designs are obtained using the hybrid approaches.

However, including two rather than one Navier-Stokes steps only gives a marginal increase in performance, NS(2)-A(4) and NS(1)-A(5), respectively. Likewise, it is seen that running three rather than two Navier-Stokes steps also only yields a marginal improvement. In terms of core-hours, the approximate model is extremely cheap compared to the Navier-Stokes model. The full six continuation steps only used 909 core-hours, made up of 200 cores for 4 hours and 32 minutes. In comparison, three steps using the Navier-Stokes model used 34 times as many core-hours, namely 30984 made up of 1000 cores for 31 hours. Finally, it is clear from looking at the values for NS(2)-A(4) and NS(2), that finishing off with some steps using the approximate model can improve the performance further quite significantly.

DISCUSSION AND CONCLUSIONS

The presented results indicate that the previously developed approximate flow model [20, 23] has limitations as a surrogate model for the full Navier-Stokes equations. The lack of inertia

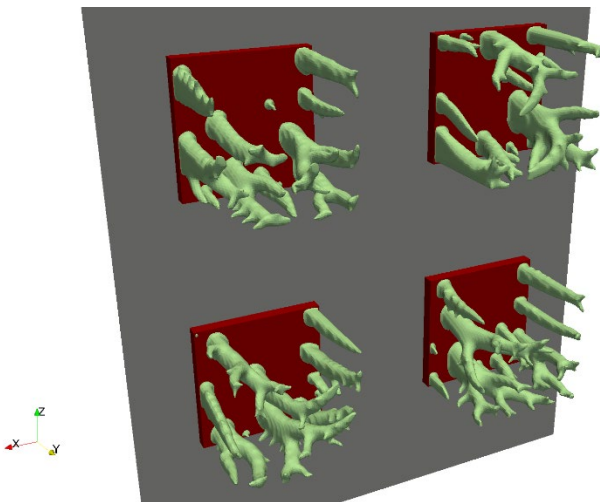


Fig. 8: Optimised heat sink designs using the NS(1)-A(5) model configuration.

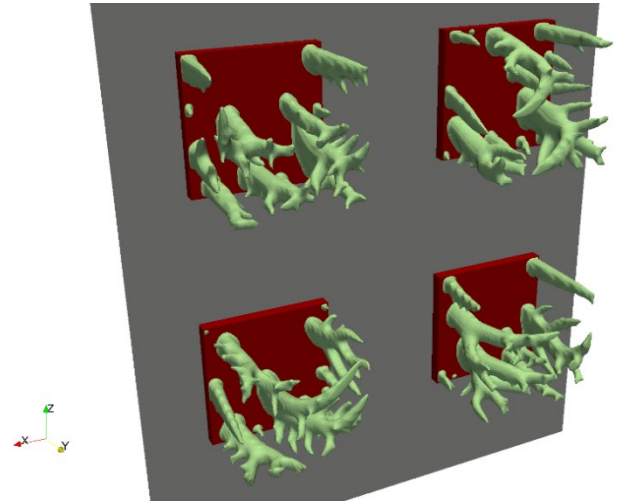


Fig. 9: Optimised heat sink designs using the NS(2)-A(4) model configuration.

and viscous boundary layers seems to be more important for the present problem because: the heat sinks are placed in an array where inertia determines which are hit by cool air; the walls of the cabinet are very close to the design domain.

However, as a supplement to the full model, the approximate model seems to have definite merits. Combined in a hybrid optimisation approach, using the full model in the beginning to point the optimisation in the right direction, the approximate model can be used in the final stages to fine tune the heat sink designs at a vastly reduced cost to using the full model all the way. It is concluded that heat sink designs should be different for each of the chips in the cabinet depending on its location and interaction with the thermal plumes from other chips.

In order to determine whether the approximate model is good enough on its own to provide something better than conventional heat sinks, future work will compare the obtained designs with optimised straight pin fin heat sinks. Furthermore, several improvements to the approximate model will be tested out to see if the accuracy can be improved. Based on the observed effects near the smooth transitional boundary of the density-based design description, it could be possible to introduce an artificial viscous boundary layer at the outer walls in a similar fashion. Lastly, the design domain will be enlarged to cover more of the fluid domain, in order to allow for the introduction of flow channels to help distribute the cool air more evenly and avoid areas of flow circulation.

ACKNOWLEDGEMENTS

The author would like to thank Nicoló Pollini for their previous joint work which laid the foundation for the present study. A portion of this work was carried out while employed at the Technical University of Denmark, for which the author thanks Professor Ole Sigmund.

REFERENCES

1. Bendsøe, M.P. and N. Kikuchi, *Generating optimal topologies in structural design using a homogenization method*. Computer Methods in Applied Mechanics and Engineering, 1988. **71**(2): p. 197-224.
2. Bendsøe, M.P. and O. Sigmund, *Topology Optimization*. 2004.
3. Deaton, J.D. and R.V. Grandhi, *A survey of structural and multidisciplinary continuum topology optimization: post 2000*. Structural and Multidisciplinary Optimization, 2014. **49**(1): p. 1-38.
4. Borrvall, T. and J. Petersson, *Topology optimization of fluids in Stokes flow*. International Journal for Numerical Methods in Fluids, 2003. **41**(1): p. 77-107.
5. Gersborg-Hansen, A., O. Sigmund, and R.B. Haber, *Topology optimization of channel flow problems*. Structural and Multidisciplinary Optimization, 2005. **30**(3): p. 181-192.
6. Olesen, L.H., F. Okkels, and H. Bruus, *A high-level programming-language implementation of topology optimization applied to steady-state Navier-Stokes flow*. International Journal for Numerical Methods in Engineering, 2006. **65**(7): p. 975-1001.
7. Dede, E.M. *Multiphysics Topology Optimization of Heat Transfer and Fluid Flow Systems*. in *COMSOL Conference 2009*. 2009. Boston.
8. Yoon, G.H., *Topological design of heat dissipating structure with forced convective heat transfer*. Journal of Mechanical Science and Technology, 2010. **24**(6): p. 1225-1233.
9. Dbouk, T., *A review about the engineering design of optimal heat transfer systems using topology optimization*. Applied Thermal Engineering, 2017. **112**: p. 841-854.
10. Alexandersen, J., et al., *Topology optimisation for natural convection problems*. International Journal for Numerical Methods in Fluids, 2014. **76**(10): p. 699-721.
11. Alexandersen, J., O. Sigmund, and N. Aage, *Large scale three-dimensional topology optimisation of heat sinks cooled by natural convection*. International Journal of Heat and Mass Transfer, 2016. **100**: p. 876-891.
12. Alexandersen, J., et al., *Design of passive coolers for light-emitting diode lamps using topology optimisation*. International Journal of Heat and Mass Transfer, 2018. **122**: p. 138-149.
13. Lazarov, B.S., et al., *Experimental validation of additively manufactured optimized shapes for passive cooling*. Applied Energy, 2018. **226**: p. 330-339.
14. Lei, T., et al., *Investment casting and experimental testing of heat sinks designed by topology optimization*. International Journal of Heat and Mass Transfer, 2018. **127**: p. 396-412.
15. Alexandersen, J., *Topology optimisation for convection problems*. 2011, Technical University of Denmark.
16. Bruns, T.E., *Topology optimization of convection-dominated, steady-state heat transfer problems*. International Journal of Heat and Mass Transfer, 2007. **50**(15): p. 2859-2873.
17. Coffin, P. and K. Maute, *Level set topology optimization of cooling and heating devices using a simplified convection model*. Structural and Multidisciplinary Optimization, 2016. **53**(5): p. 985-1003.
18. Zhou, M., et al., *Industrial application of topology optimization for combined conductive and convective heat transfer problems*. Structural and Multidisciplinary Optimization, 2016. **54**(4): p. 1045-1060.
19. Alexandersen, J., *Efficient topology optimisation of multiscale and multiphysics problems*. 2016, Technical University of Denmark.
20. Asmussen, J., et al., *A "poor man's" approach to topology optimization of natural convection problems*. Structural and Multidisciplinary Optimization, 2019. **59**(4): p. 1105-1124.
21. Joo, Y., I. Lee, and S.J. Kim, *Efficient three-dimensional topology optimization of heat sinks in natural convection using the shape-dependent*

- convection model*. International Journal of Heat and Mass Transfer, 2018. **127**: p. 32-40.
22. Joo, Y., I. Lee, and S.J. Kim, *Topology optimization of heat sinks in natural convection considering the effect of shape-dependent heat transfer coefficient*. International Journal of Heat and Mass Transfer, 2017. **109**: p. 123-133.
23. Pollini, N., et al., *A “poor man’s” approach for high-resolution three-dimensional topology design for natural convection problems*. Advances in Engineering Software, 2020. **140**: p. 102736.
24. Bourdin, B., *Filters in topology optimization*. International Journal for Numerical Methods in Engineering, 2001. **50**(9): p. 2143-2158.